Carbon and oxygen net community production in the eastern tropical Atlantic estimated from a moored buoy

Nathalie Lefèvre, Liliane Merlivat

Carbon and oxygen net community production in the eastern tropical Atlantic estimated from a moored buoy

Nathalie Lefèvre[1] and Liliane Merlivat[1]

Received 14 December 2010; revised 7 June 2011; accepted 1 November 2011; published 24 January 2012.

[1] A mooring at 6°S, 10°W has been equipped with an oxygen optode and a Carioca sensor for monitoring hourly oxygen (O_2) and the fugacity of CO_2 (fCO_2) at 1.5 m depth since June 2006. Due to biofouling, the oxygen time series lasted between 72 days in 2008 to 159 days in 2009. Using an alkalinity-salinity relationship determined for the area, dissolved inorganic carbon (DIC) is calculated. Short-term and long-term net community productions (NCP) are calculated using a mass balance approach for DIC and O_2 under the assumption of no mixing conditions. The mooring site is always supersaturated in oxygen except in 2007 when depleted oxygen waters are observed from June to September, during the upwelling season. Averaging all the short time events, NCP calculated from the rates of changes of O_2 and DIC leads to a NCP of 16.6 $\pm$ 6.1 mmol C $m^{-2}d^{-1}$, ranging from 14.7 mmol C $m^{-2}d^{-1}$ in 2008 to 17.4 mmol C $m^{-2}d^{-1}$ in 2006. The mean daily oxygen biological production rate determined over the whole time series shows a significant year to year variability with 7.5 mmol C $m^{-2}d^{-1}$ in 2008 to 15.6 mmol C $m^{-2}d^{-1}$ in 2009. A photosynthetic quotient ranging between 1.0 to 1.3 has been determined when both carbon and oxygen NCP values are available.

Citation: Lefèvre, N., and L. Merlivat (2012), Carbon and oxygen net community production in the eastern tropical Atlantic estimated from a moored buoy, *Global Biogeochem. Cycles*, *26*, GB1009, doi:10.1029/2010GB004018.

1. Introduction

[2] The net community production (NCP) is an important aspect of the carbon cycle because the biological consumption of carbon decreases the surface fugacity of CO_2 (fCO_2) and hence, alters the air-sea exchange of CO_2. NCP measures the biota contribution to the marine carbon cycle.

[3] Because of the difficulty of measuring NCP, there are not many measurements available and current NCP rates are poorly known in many regions of the ocean [*Quay et al.*, 2010]. In addition, the processes that regulate NCP, gross primary production (GPP) and respiration (R) are poorly understood. The traditional method of determining NCP is by measuring gross production and respiration from in vitro changes of dissolved oxygen using light and dark incubators. NCP has also been determined by the means of geochemical budgets using oxygen or dissolved inorganic carbon [*Neuer et al.*, 2007]. The similar solubility of oxygen and argon (Ar) gases has been used to determine NCP as Ar is not involved in biological processes unlike O_2 [e.g., *Emerson et al.*, 1997; *Kaiser et al.*, 2005; *Luz and Barkan,* 2009; *Quay et al.*, 2010]. The pair O_2/N_2 has also been used although the solubility of nitrogen gas is different from the one of oxygen [e.g., *Emerson et al.*, 2008].

[4] However, geochemical and biological approaches give different estimates of NCP, which leads to uncertainties about the metabolic state of the ocean [*Karl et al.*, 2003]. Tropical and subtropical area are remineralization intensive systems [*Quay et al.*, 2010], therefore, GPP is close to R and errors can be made more easily about the autotrophy or heterotrophy of such systems. *Mouriño-Carballido and Anderson* [2009] determined NCP using in vitro and in situ 1-D modeling techniques and found that in vitro estimates were systematically lower than the model-derived techniques so that heterotrophy was observed with in vitro estimates but not with the model derived estimates in the Sargasso Sea. The geochemical approach integrates NCP over larger temporal and spatial scales than bottle measurements made over a few hours at a given location. This is one possible explanation for the discrepancy between the NCP estimates given by the two approaches. Methodological artifacts associated with in vitro techniques have also been suggested as another explanation [e.g., *Mouriño-Carballido and Anderson*, 2009; *Quay et al.*, 2010].

[5] The knowledge of NCP in tropical areas is also of interest because, although NCP fluxes are relatively small in these regions, they correspond to large area of the ocean so the biological consumption of carbon can represent an important fraction of the ocean carbon biological pump.

[6] The aim of the present work is to provide new NCP measurements in the eastern tropical Atlantic (6°S, 10°W) based on continuous time series of physical and chemical data measured on a moored buoy over the period 2006–2009. This paper provides an in situ estimation of net community

[1]LOCEAN, UMR7159, Université Pierre et Marie Curie, CNRS, IRD, MNHN, Paris, France.

0886-6236/12/2010GB004018

Table 1. Dates of Oxygen Data Availability, Number of Days of the Time Series, DIC Data Availability, Number of Days, and Corresponding SST (in °C) and SSS Averaged Over the Oxygen Data Period With One Standard Deviation

Year	Period for O_2	Number of Days	Period for DIC	Number of Days	⟨SST⟩	⟨SSS⟩
2006	8 Jun to 27 Aug	84	8 Jun to 31 Dec	206	25.62 ± 0.99	35.972 ± 0.159
2007	29 Jun to 15 Sep	78	1 Jan to 13 Oct	286	24.71 ± 0.63	35.775 ± 0.174
2008	17 Sep to 28 Nov	72	17 Sep to 31 Dec	105	24.52 ± 0.27	36.100 ± 0.058
2009	11 Jul to 17 Dec	159	11 Jul to 17 Dec	159	24.36 ± 0.46	35.835 ± 0.194

production based on carbon and oxygen measurements. The carbon estimated NCP is based on the analysis of the distribution of dissolved inorganic carbon (DIC) calculated from hourly records of fCO_2 at the ocean surface (1.5 m depth) as done by *Parard et al.* [2010]. Here, we focus on oxygen measurements. An oxygen mass balance approach is used to estimate NCP that is directly comparable to the carbon-based NCP values, and to calculate a mean daily oxygen biological production over the duration of the time series. The results are then discussed and compared with previous estimates of NCP for the tropical and subtropical ocean.

2. Data and Methods

2.1. Data at the Mooring Site

[7] A CARIOCA CO_2 sensor and an Aanderaa 3830 optode have been installed on the 6°S, 10°W buoy [*N. Lefèvre et al.*, 2008] of the PIRATA (Prediction and Research Moored Array in the Tropical Atlantic) network since June 2006. One objective of this network of moored buoys is to monitor the ocean circulation [*Bourlès et al.*, 2008]. Each buoy is equipped with Seabird sensors for measuring temperature and salinity at different depths. Wind speed is recorded at a height of 4 m. At 6°S, 10°W, ocean temperature is measured at 1.5 m, 20 m, 40 m, 60 m, 80 m, 100 m, 120 m, 140 m, 180 m, 300 m and 500 m. Salinity is measured at 1.5 m, 20 m, 40 m and 120 m. Because of the coarser vertical resolution of salinity measurements, the mixed layer depth is estimated from the temperature profiles at the mooring. Mixed layer depths are also calculated from ARGO floats which were within ±100 km and ±10 days of the mooring. There was no ARGO float meeting these criteria in 2007 and in 2008. The mixed layer depth is estimated when the temperature gradient from the surface exceeds 0.1°C.

[8] The fugacity of CO_2, the dissolved oxygen concentration, the sea surface temperature and the sea surface salinity are measured at a depth of 1.5 m on an hourly basis and are transmitted by Argos. Atmospheric pressure is also measured. The CO_2 sensor and the oxygen optode are replaced every year during the cruise servicing the PIRATA moorings. The dates of the replacement are 8 June 2006, 29 June 2007, 17 September 2008 and 11 July 2009. The fCO_2 data from 2006 to 2009 have been published by *Parard et al.* [2010]. The first sensor lasted one year but electronic or mechanical failures explain the different lengths of the time series. In 2008 and 2009, the time series are much shorter (Table 1). Total alkalinity was estimated from salinity using seawater samples taken in this region. The error on predicted alkalinity is ±11 μmol/ kg [*N. Lefèvre et al.*, 2008]. Dissolved inorganic carbon was then calculated from fCO_2, TA, SST and SSS using the dissociation constants of *Mehrbach et al.* [1973] refitted by *Dickson and Millero* [1987]. An error of 1 μmol kg^{-1} on TA leads to an error of 0.8 μmol kg^{-1} on DIC so our value of DIC is accurate at ±8.8 μmol kg^{-1}.

2.2. Oxygen Measurements

[9] The oxygen optode is calibrated in fresh water in the laboratory before deployment using a zero and 100% oxygen reference points. No drift is detected when the optode is retrieved. However, absolute oxygen values can be different from the oxygen measurements made by the Winkler method. Therefore, the optode data are calibrated against the Winkler measurements made during the cruise for servicing the mooring. A constant offset was applied to correct the data. *Johnson* [2010] compared the optode measurements recorded at a time series off Monterey Bay, California, with shipboard measurements made using the Winkler method. He found an offset between the two techniques, but it remained constant over the 5 months period of his record.

[10] Oxygen saturation, $O_{2\,sat}$ (in μmol kg^{-1}) is calculated using the equation of *García and Gordon* [1992]. The degree of O_2 saturation, in percent, is given by:

$$\%\ O_2\ \text{sat} = ([O_2]/[O_{2\text{sat}}]) \times 100 \quad (1)$$

Over time, a sudden increase of the amplitude of the diurnal signal, and sometimes a drift toward lower oxygen values as well, are a signature of biofouling of the sensor. For example, in 2006, a clear degradation of the oxygen signal occurs from the 27th of August with an amplitude of the diurnal cycle greater than 10 μmol kg^{-1} (Figure 1). Thus, the length of the time series ranges from 72 days in 2008 to 159 days in 2009 (Table 1). In 2009, the oxygen record was interrupted

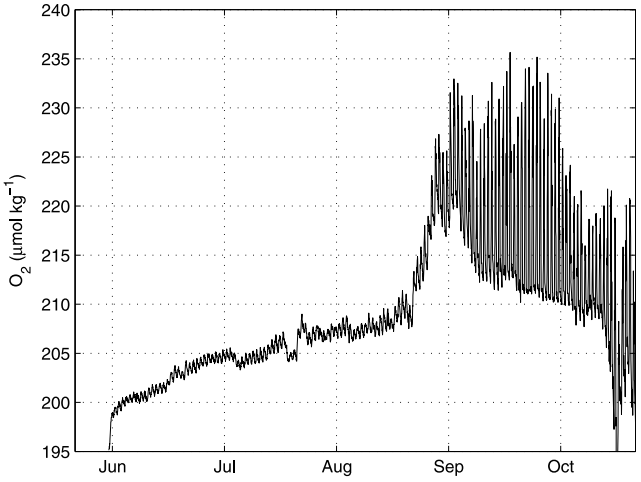

Figure 1. Variability of the dissolved oxygen concentration between the 8th of June and the 27th of October 2006.

because of the general failure of the electronics of the system (seawater in the system), but no biofouling was observed over the 159 period, probably because of the addition of a copper mesh on the optode. Although copper reacts with seawater and can modify the pH, we did not find any significant difference between optode measurements with or without the copper mesh from experiments done in laboratory. In 2008, a shift of oxygen data of 18 μmol kg^{-1} in four days has been observed, after a period of 10 days, without any sign of biofouling. The shift might have been caused by an electronic interference as the amplitude of the diurnal cycle is correct. The data corresponding to the shift were disregarded. There is neither an increase of diurnal amplitude nor a drift. Therefore, we simply apply an offset of 18 μmol kg^{-1} to the data. After applying this offset, the November 2008 data are in good agreement with the November 2006 Winkler value.

2.3. Calculation of Air-Sea Fluxes

[11] The air-sea CO_2 flux is calculated in mmol m^{-2}d^{-1} by the following equation:

$$F_{CO2} = k_{CO2}\,\alpha_{CO2}(fCO_{2sea} - fCO_{2atm}) \quad (2)$$

where α_{CO2} is the solubility of CO_2 [*Weiss*, 1974], fCO_{2sea} the fugacity of CO_2 in seawater (in μatm), fCO_{2atm} the fugacity of CO_2 in the atmosphere and k_{CO2} is the gas transfer velocity (in m d^{-1}) for CO_2. fCO_{2atm} is computed from the monthly molar fraction xCO_2 at the atmospheric station at Ascension Island (7.92°S, 14.92°W) of the NOAA/ESRL Global Monitoring Division (http://esrl.noaa.gov/gmd/ccgg/iadv), the water vapor pressure of *Weiss and Price* [1980] and the atmospheric pressure recorded at the mooring.

[12] Injection of air bubbles below the air-water interface is neglected for the calculation of the CO_2 flux but this contribution to the flux can be relatively important for oxygen as it is a less soluble gas. The equation of the O_2 flux is then given by:

$$F_{O2} = k_{O2}\,\rho([O_2] - [O_{2\,sat}]) - F_{bub} \quad (3)$$

where k_{O2} is the gas transfer velocity (in m d^{-1}), ρ is the density of seawater (in kg m^{-3}) and F_{bub} is the contribution of air bubbles calculated with the formula given by *Woolf and Thorpe* [1991]:

$$F_{bub} = k_{O2}\ \rho\ 0.01\ \left(U/U_0\right)^2\ [O_{2\ sat}] \quad (4)$$

where U is the wind speed at 10m height in ms^{-1} and U_0 a model-derived constant for O_2 of 9 ms^{-1}. *Mouriño-Carballido and Anderson* [2009] showed that this bubble flux formula gave similar results to the formula used by *Stanley et al.* [2009]. The total oxygen flux becomes:

$$F_{O2} = k_{O2}\ \rho\ \left([O_2] - [O_{2\ sat}]\ \left(1 + 1.23\ 10^{-4}\ U^2\right)\right) \quad (5)$$

It results from this equation that the flux is positive when there is outgassing to the atmosphere. The fluxes are expressed in mmol m^{-2}d^{-1}.

[13] For both CO_2 and O_2, the gas transfer velocity (in cm/h) is calculated using the formula of *Sweeney et al.* [2007]:

$$K = 0.27\ U^2\ (660/Sc)^{0.5} \quad (6)$$

where Sc is the Schmidt number, Sc_{CO2}, for CO_2 or Sc_{O2} for O_2 [*Wanninkhof*, 1992].

[14] The daily wind speed recorded at the mooring at 4 m is converted to a 10 m wind speed and interpolated at hourly scale to compute hourly fluxes.

2.4. Calculation of in Situ Net Community Production

[15] NCP has been previously calculated, at daily scale, from daily cycles of DIC on drifting Carioca buoys [*Boutin and Merlivat*, 2009; *Merlivat et al.*, 2009].

[16] Depending on atmospheric forcing conditions, a warm diurnal layer can be formed during the daylight period [e.g., *McNeil and Farmer*, 1995; *Merlivat et al.*, 2009; *Wade et al.*, 2011]. In particular, it was evidenced at the PIRATA moorings at 10°W [*Wade et al.*, 2011]. In this surface layer, biological activity occurs from the sunrise to the sunset. During daytime, DIC decreases and O_2 increases due to production. DIC reaches a minimum and O_2 a maximum when respiration compensates production. At night, the mixed layer deepens and maximum of DIC and minimum of O_2 are observed mainly at the end of nocturnal convection.

[17] Biological processes, i.e., photosynthesis and respiration, and air-sea exchange are the mechanisms responsible for the change in DIC and O_2 during the daylight period at the sampling depth of the water, 1.5 m. This assumes that mixing due to lateral advection is negligible, and that no vertical supply occurs during daylight as the mixed layer is shoaling. At night, convection mixes the warm layer, established during daylight, down to the lower levels of the MLD, bringing cold deeper water, richer in DIC, to the surface.

[18] ΔDIC_{Max} is the change of the maximum of DIC computed across two consecutive mornings at the end of the nocturnal convection within the mixed layer (thickness h) as done by *Parard et al.* [2010]. Net community production and air-sea exchange over one day within the mixed layer are the processes responsible for these changes of DIC:

$$\frac{\Delta DIC_{\mathrm{Max}}}{\Delta t} = NCP_h - \frac{1}{\rho}\frac{F_{CO2}}{h} \quad (7)$$

where ρ is the density of seawater (in kg m^{-3}), NCP_h is the net community production of carbon in the mixed layer (in μmol kg^{-1}).

[19] The oxygen concentration in the surface layer is affected by air-sea exchange, injection of air bubbles, entrainment of water from below during mixed layer deepening, lateral advection from surrounding waters and biological activity. Horizontal advection can be neglected for oxygen because of the rapid exchange with the atmosphere. Therefore, a one dimensional model is assumed and the change of mixed-layer oxygen concentration as a function of time can be written as follows:

$$\frac{h\ d[O_2]}{dt} = -k_{O_2}\rho([O_2] - [O_{2sat}]) + F_{bub} + \frac{dh}{dt}\left([O_2]_{sub} - [O_2]\right) + J \quad (8)$$

where h is the mixed layer depth in m, $[O_2]_{sub}$ is the oxygen concentration below the mixed layer and J is the biological production in mol m^{-2}d^{-1}.

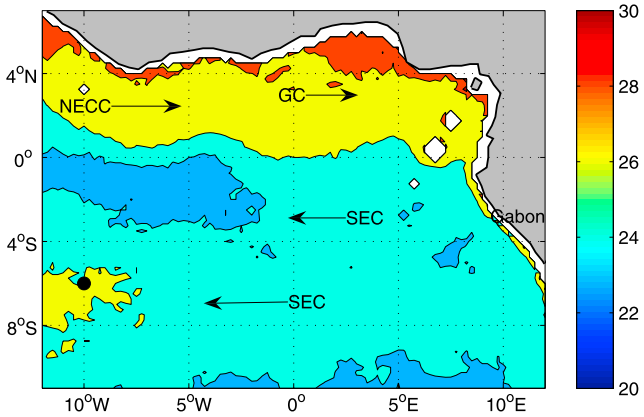

Figure 2. Three day composite of SST of 1 July 2006 from the TRMM (Tropical Rain Mission Measurements) Microwave Imager (TMI) with location of the mooring at 6°S, 10°W.

[20] Assuming a photosynthetic quotient, PQ, equal to 1.4 [*Laws*, 1991], NCP expressed in mmol C $m^{-2}d^{-1}$ is given by:

$$NCP = -NCP_{O2}/1.4 \quad (9)$$

As a decrease of DIC due to biological processes does not change alkalinity significantly, a change of alkalinity (i.e., salinity) is the result of advection. Therefore, alkalinity is used to check the assumption of no advection made for this calculation.

3. Processes Affecting the O_2 and CO_2 Distribution

[21] The mooring at 6°S, 10°W is located in the westward-flowing South Equatorial Current (SEC). The equatorial upwelling is further north (0–4°S) of the mooring and the coastal Congo-Gabon upwelling is further east. These two upwellings merge and form a cold tongue that propagates within the SEC, which explains the lower temperature recorded at the mooring [*N. Lefèvre et al.*, 2008; *Parard et al.*, 2010]. The Atlantic cold tongue develops between June to October from the African coast to about 20°W and shows some spatial and temporal variability [*Caniaux et al.*, 2011]. The satellite image of SST for July 2006 highlights the propagation of the cold tongue with cold water of the equatorial upwelling and cold water coming from the eastern southern part of the region and merging with the equatorial upwelling (Figure 2).

[22] The optode worked for different periods of time, between June and December, from 2006 to 2009 (Table 1). Over the length of each time series, the mean surface temperature and salinity are not significantly different from one year to another. The amplitude of the seasonal cycle at this site is relatively small with an average of 5°C.

[23] The oxygen distribution at 6°S, 10°W varies from year to year with lower values observed in June and higher values from September to December (Figure 3a). The amplitude of oxygen variations is rather small with a value of 21 μmol/kg in 2006, and a maximum of 31 μmol/kg over all the years. In 2009, when the longest record of oxygen data is obtained, the difference between the maximum and the minimum oxygen values is less than 15 μmol/kg.

[24] The mooring site is mostly supersaturated in oxygen, except in 2007 when the water is undersaturated from June to September (Figure 3b) during the upwelling season. Oxygen increases are caused by biological activity. Upwelling regions are usually characterized by oxygen undersaturation [e.g., *Garcia and Keeling*, 2001; *Najjar and Keeling*, 2000] because the subsurface layers, brought to the surface, are oxygen depleted due to respiration and remineralization. However, there is no evidence of a stronger upwelling in 2007 compared to 2006 and 2008 [*Caniaux et al.*, 2011] that could explain the undersaturation in 2007. This might be due to a bias in the optode data but the oxygen measurements made during the cruise also show lower oxygen values in 2007.

[25] Although strong horizontal gradients of temperature are observed during the propagation of the cold tongue [*Caniaux et al.*, 2011], the oxygen distribution does not exhibit large variations. From June to September, SST decreases by more than 3°C due to the propagation of the cold tongue but the oxygen concentration increases. However, the propagation of upwelled waters should lead to a decrease of oxygen as they have lower oxygen content than surface waters. This suggests that rapid oxygen exchange occurs with the atmosphere and counterbalances the decrease of oxygen due to the propagation of upwelled waters. Thus, the impact of horizontal advection can be neglected. This assumption was also made at the Hawaii Ocean time series station [*Emerson et al.*, 2008]. At other mooring sites, horizontal advection can be significant. For example, at station P, *Emerson and Stump* [2010] reported strong horizontal gradients.

[26] For fCO_2 and DIC, horizontal advection cannot be neglected, the cold tongue supplies CO_2 rich waters and gas exchange is not fast enough to obtain an fCO_2 close to equilibrium conditions. During the upwelling season, fCO_2 increases. In 2006, fCO_2 varied by 90 μatm and DIC by 70 μmol/kg [*Parard et al.*, 2010]. On the contrary, the amplitude of the oxygen concentration remains small, less than 10 μmol/kg.

[27] Oxygen concentrations always increase from June to September during the propagation of the cold tongue when SST decreases. This suggests that biological activity dominates during the upwelling season. Different water masses are observed at the mooring and explain the variability of the sea surface salinity (Figure 3d). The high frequency variability of the oxygen and SST data are caused by the diurnal cycle.

[28] The maximum of solar radiation is observed around 12–13 h local time. The SST maximum is delayed by about 2 h, which corresponds to the time it takes to warm up the mixed layer. In some cases, such as the period from 6 to 11 July 2006, the oxygen maximum is associated with the SST maximum (Figure 4a). Other processes counterbalance the biological processes on the DIC distribution. During the upwelling season, lateral advection is significant because of the propagation of the cold tongue, rich in CO_2. A diurnal cycle of oxygen can be observed without a clear DIC signal associated with it. Some periods of the time series are characterized by a maximum of O_2 occurring about two hours after the maximum of SST, as illustrated by the distribution of O_2 and SST during the 12–16 August 2006 period (Figure 4b). However, the time series shows a broad maximum of oxygen during the daylight period consistent

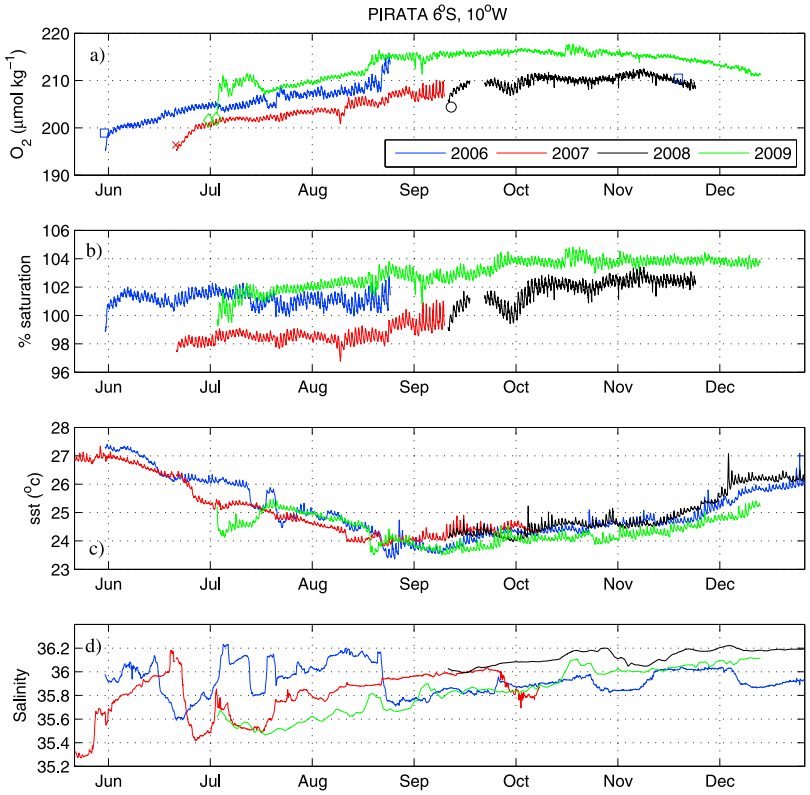

Figure 3. Variability of (a) dissolved oxygen, (b) oxygen saturation, (c) SST and (d) surface salinity at 6°S, 10°W as a function of time. The squares, cross, circle and diamonds correspond to the oxygen data made by Winkler titration in 2006, 2007, 2008 and 2009 respectively.

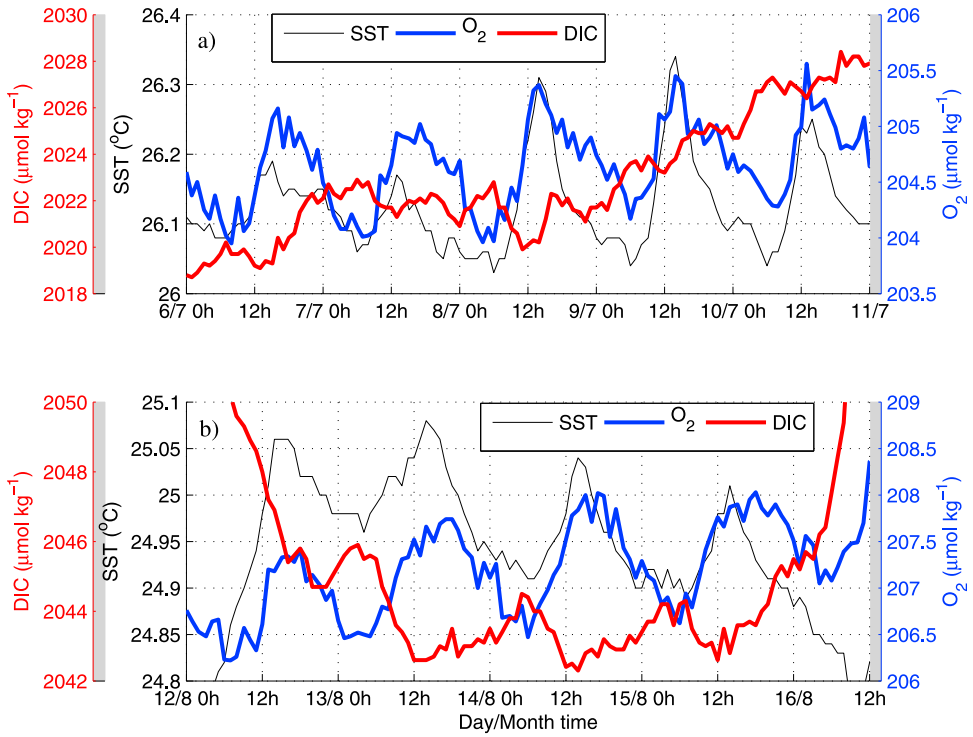

Figure 4. Diurnal cycles of SST, O_2 and DIC for (a) 6–11 July 2006 and (b) 12–16 August 2006 as a function of the day and time of the year.

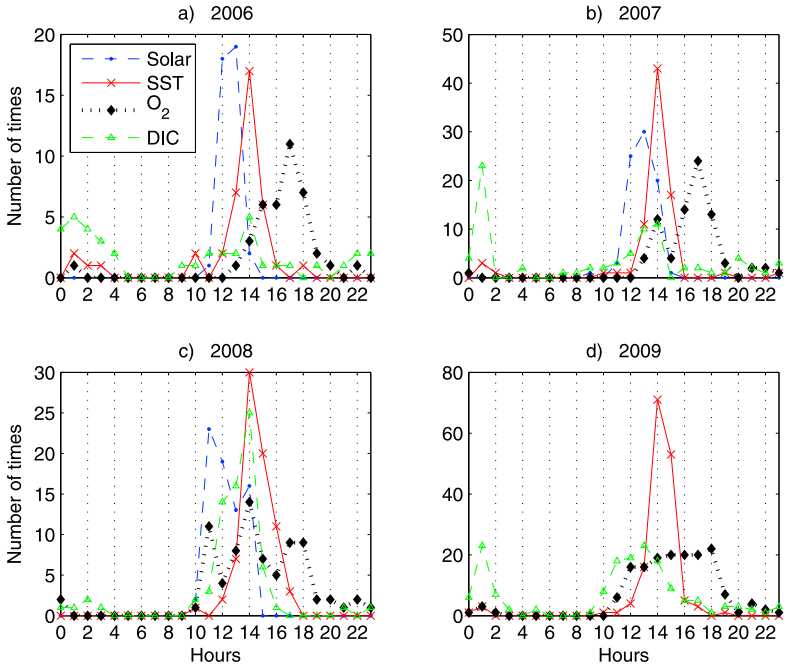

Figure 5. Number of occurrences of the daily maximum of O_2 (dotted line with diamonds, in black), maximum of solar radiation (dash dotted line, in blue), maximum of SST (solid line with crosses, in red), minimum of DIC (dash line with triangles, in green) as a function of the hour of the day for (a) 2006, (b) 2007, (c) 2008 and (d) 2009.

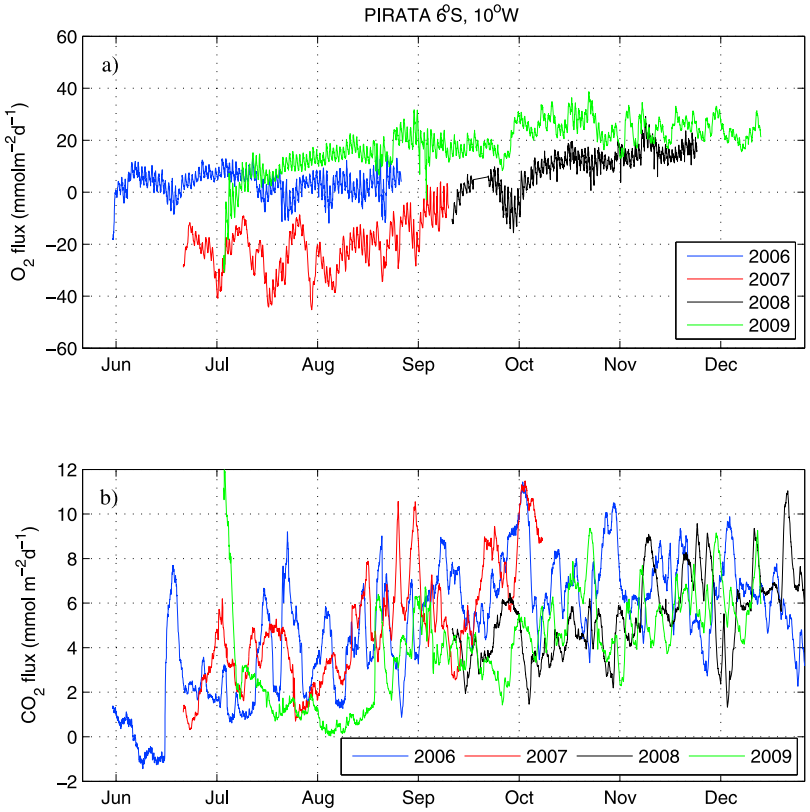

Figure 6. (a) Air-sea fluxes of O_2, including the bubbles contribution, from 2006 to 2009 as a function of time. A positive flux corresponds to outgassing of O_2. (b) Air-sea fluxes of CO_2 from 2006 to 2009 (positive for outgassing).

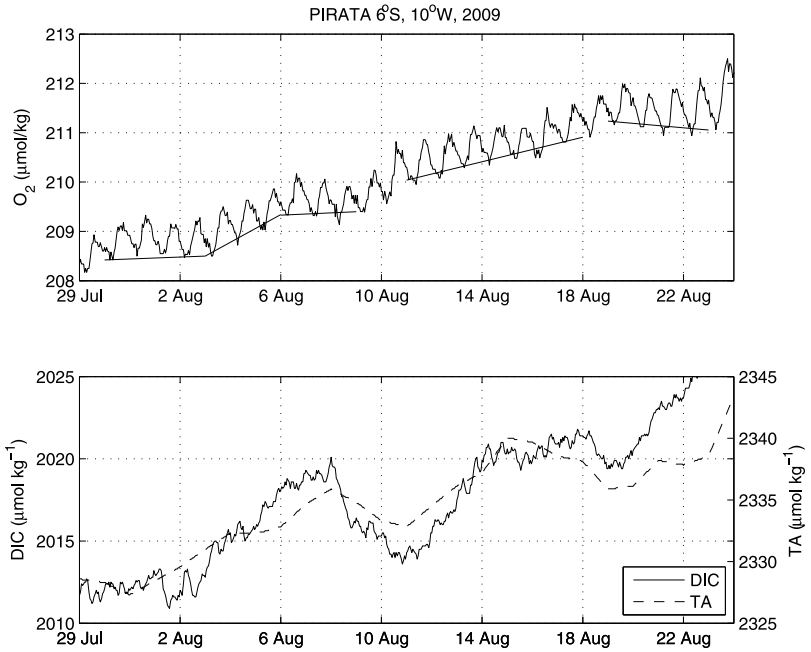

Figure 7. (top) O_2 distribution between 29 July and 23 August 2009 at the 6°S, 10°W site. The solid lines correspond to the variations of the minima of O_2 over the 30 July–3 August, 3–6 August, 6–9 August, 11–18 August and 19–23 August 2009 periods. (bottom) DIC (solid line) and alkalinity (dash line) distributions over the same period as O_2.

with production by biological activity. During that August period, a diurnal cycle of DIC is observed with a minimum of DIC close to the time of the maximum of O_2.

[29] Using the data over the periods of available oxygen for the years 2006 to 2009, the daily maxima of O_2, SST and solar radiation, and the daily minimum of DIC are determined and the number of occurrences of these extrema are plotted as a function of the hour of the day for each time series (Figure 5). In 2009, there are no solar radiation measurements. The maximum of O_2 occurs mostly at 16 h while the maximum of SST is at 14 h, 7.5 h after sunrise and two hours after the maximum of solar radiation (Figure 5). There is no clear minimum of DIC except in 2008 when the minimum occurs mostly at 14 h at the time of the maximum SST. This suggests that the biological processes during daylight are less pronounced on DIC compared to O_2. In 2008, the period of measurements is after the upwelling season, from mid-September onwards. Therefore, lateral advection is less important than during the propagation of the cold tongue. This might explain why the DIC signal is more visible in 2008, compared to the other years, with a minimum broadly coinciding with the oxygen maximum.

[30] In addition to convection and biological activity, gas exchange affects both O_2 and CO_2 (hence DIC). O_2 exchanges more rapidly with the atmosphere than CO_2 so differences between DIC and O_2 could be due to the different time constants of the processes involved. The oxygen flux, including the contribution of bubbles, is about ten times larger than the air-sea CO_2 flux (Figure 6) and the diurnal cycle is visible (Figure 6a). A sensitive study can be done to evaluate the impact of air-sea gas exchange on the diurnal cycling of O_2 and DIC. Under the assumption of no mixing, and using the relationship between the NCP based on O_2 and carbon (equation (9)), the mass balance equations for O_2 and DIC become:

$$h\frac{dDIC}{dt} = NCP - F_{CO2} \tag{10}$$

$$h\frac{dO_2}{dt} = -1.4\,NCP - 10\,F_{CO2} \tag{11}$$

Assuming a mean F_{CO2} of 5 mmol $m^{-2}d^{-1}$ and a mean NCP of 20 mmol $m^{-2}d^{-1}$, and after taking the ratio of these equations, a relationship between the O_2 and DIC variations is obtained:

$$\frac{dO_2}{dt} = -5\,\frac{dDIC}{dt} \tag{12}$$

The amplitude of the diurnal changes of oxygen is about 5 times greater than those of DIC if we take into account the impact of the gas exchange only.

[31] The oxygen flux is mostly toward the atmosphere (positive values) except in 2007 when it is into the ocean. The mooring site is a source of CO_2 except in June 2006 where a slight undersaturation is observed before the propagation of the cold tongue that supplies CO_2 rich waters.

4. Quantification of Biological Processes

4.1. In Situ Net Community Production

[32] When alkalinity variations are less than 1 μmol/kg, we assume that lateral advection and vertical mixing can be neglected. Net community production is calculated using the mass balance equations for DIC and O_2 (equations (7) and (8)) for short-term biological events. For each year,

Table 2. Periods Identified for Calculating NCP From an Increase of Minima in O_2 or a Decrease of Maxima in DIC[a]

Period	dO_{2Min}/dt	FO_2	$dDIC_{Max}/dt$	FCO_2	MLD	NCP
10–14 Jun 2006	0.33	3.2			60	16.2
29 Jun to 5 Jul 2006	0.21	5.3			60	12.8
19–25 Jul 2006	0.31	1.1			60	14.0
31 Jul to 3 Aug 2006	0.25	1.6			60	11.7
12–17 Aug 2006	0.17	−1.7			60	8.3
20–26 Aug 2006	0.25	1.4			60	11.6
16–19 Sep 2006			−0.65	7.3	50	26
22–30 Sep 2006			−0.5	5.4	50	20.2
17–19 Oct 2006			−0.65	8.1	50	25.2
1–3 Nov 2006			−0.75	9.5	50	28.9
16–19 Dec 2006			−0.56	6.4	40	16.5
2–7 Mar 2007			−0.76	6.0	40	25.1
5–9 Jul 2007	0.11	−24.8			40	−14.0
22–27 Jul 2007	0.11	−34.4			40	−20.9
30 Jul to 4 Aug 2007	0.28	−14.6			40	−5.5
19–23 Aug 2007	0.21	−19.3			40	−7.5
31 Aug to 5 Sep	0.14	−13.7			40	−5.2
6–13 Oct 2008	0.38	3.1	−0.41	3.7	50	15.6/17.3
29 Oct to 2 Nov 2008	0.27	11.1			40	15.5
7–13 Nov 2008	0.06	14.5			40	10.3
25–31 Jul 2009	0.25	8			40	12.7
30 Jul to 3 Aug 2009	0.02	11.3			40	8.4
3–6 Aug 2009	0.28	11.8			60	20.2
6–9 Aug 2009	0.01	12.9			60	9.4
11–18 Aug 2009	0.12	15.6			60	15.3
19–23 Aug 2009	−0.04	15.1			60	8.6
16–20 Oct 2009	−0.15	27.1			60	12.7
7–9 Nov 2009	0.16	23.9			40	24.1
11–14 Nov 2009	0.03	27.1	−0.75	6.8	40	19.9/23.9

[a]The rate of changes, dO_{Min}/dt and $dDIC_{Max}/dt$, are expressed in μmol $kg^{-1}d^{-1}$. FO_2 and FCO_2 correspond to the air-sea O_2 and CO_2 flux respectively (in mmol $m^{-2}d^{-1}$). The flux is positive for outgassing. MLD is the mixed layer depth (in m) and NCP is the net community production in mmol C $m^{-2}d^{-1}$. A photosynthetic quotient of 1.4 has been used to convert NCP calculated in mmol O_2 $m^{-2}d^{-1}$ to NCP in mmol C $m^{-2}d^{-1}$.

periods of several days are identified when the criteria of no advection and biological drawdown are met, which corresponds to short-term events. The air-sea flux is calculated and the mixed layer is determined from the temperature profiles at the PIRATA mooring or nearby Argo floats. A zoom for the month of August 2009 illustrates how the biological periods are detected from the hourly distributions of O_2 and DIC (Figure 7).

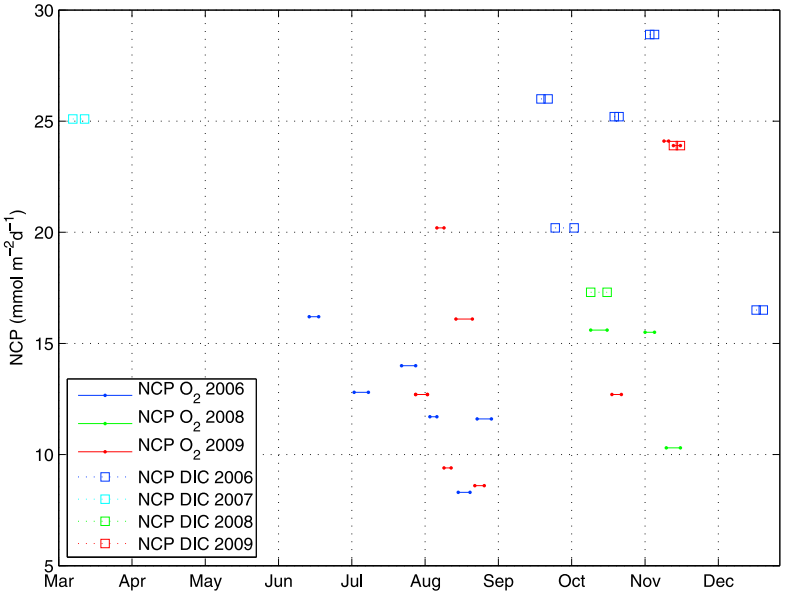

Figure 8. Net Community Production (in mmol $m^{-2}d^{-1}$) calculated over different periods using either O_2 (NCP O_2) or DIC (NCP DIC) data. The color code corresponds to the year of measurements (blue for 2006, cyan for 2007, green for 2008 and red for 2009). The length of the horizontal bar corresponds to the number of days used for the calculation.

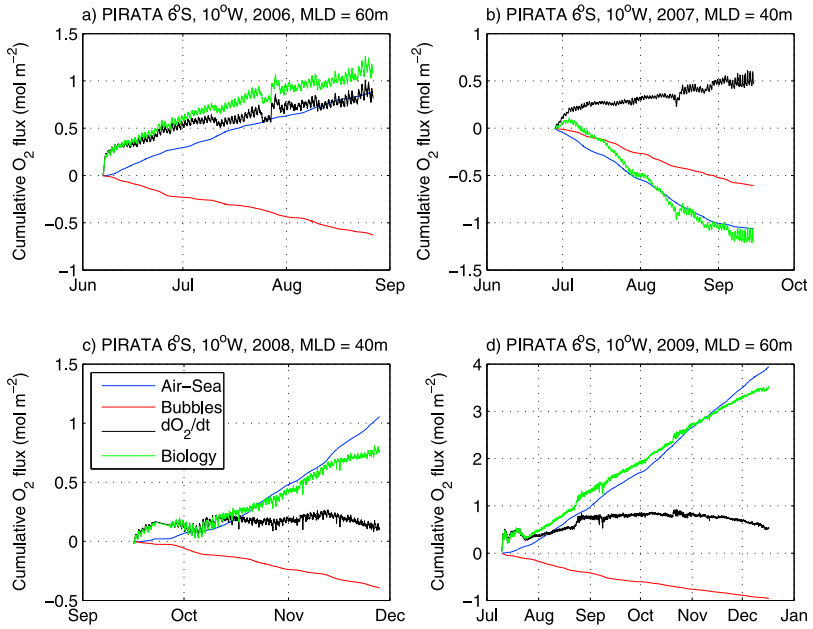

Figure 9. Cumulated biological oxygen production (in mol m^{-2}) calculated from equation (8) for (a) 2006, (b) 2007, (c) 2008 and (d) 2009 with a mixed layer depth (MLD) of 60 m, 40 m, 40 m and 60 m respectively. The time rate of change of oxygen (in black), the air-sea flux (in blue), the bubble flux (in red) and the biological flux (in green) are indicated.

[33] Over the periods of 3–6 August and 11–18 August 2009, a regular increase of O_2 is detected (Figure 7, top). Over the 30 July–3 August and 6–9 August periods, notwithstanding a clear daylight biological activity as indicated by the diurnal cycle of O_2, the O_2 minimum is almost constant (Figure 7, top). This indicates that the amount of O_2 produced by the biological processes just compensate the loss by air-sea exchange. The DIC variability over the August month is different from the O_2 distribution (Figure 7, bottom). While over the period 11–18 August, the O_2 measurements indicate a significant biological activity, DIC at the opposite increases. During that period, alkalinity (estimated from salinity) increases as well, which suggests that mixing with another water mass occurs. This is probably due to horizontal advection that affects the DIC distribution to a greater extent than the oxygen distribution. As previously reported [e.g., *Emerson and Stump*, 2010], lateral advection is of minor importance to the mass balance of major atmospheric gases except CO_2. After examining the entire time series, several periods of diurnal cycles could be identified and NCP could be calculated from either the increase of O_2 minima or a decrease of DIC maxima over time (Table 2). As expected, NCP is more frequently calculated from O_2 than from DIC (Figure 8), even though the time series for DIC is longer than for O_2, because of the smaller impact of advection on oxygen compared to DIC. A few NCP values could be calculated from DIC mainly after the upwelling season when advection is weaker. During the 6–13 October 2008 and 11–14 November 2009, NCP could be determined from both O_2 and DIC. For the periods in 2007, the NCP is negative (Table 2) because of the negative air-sea flux of O_2. With the exception of this period, the NCP values range between 8.3 and 28.9 mmol C $m^{-2}d^{-1}$ and NCP calculated from O_2 is in reasonable agreement with those calculated from DIC but slightly lower. Excluding the NCP values of 2007, the mean NCP based on O_2 calculation is 13.7 ± 4.4 mmol C $m^{-2}d^{-1}$ is slightly lower than the NCP based on carbon calculation of 22.9 ± 4.4 mmol C $m^{-2}d^{-1}$. This leads to an overall NCP of 16.6 ± 6.1 mmol C $m^{-2}d^{-1}$ with 17.4 ± 6.8 mmol C $m^{-2}d^{-1}$ in 2006, 14.7 ± 3.0 mmol C $m^{-2}d^{-1}$ in 2008 and 15.5 ± 6.1 mmol C $m^{-2}d^{-1}$ in 2009. Except for the year 2007 that is very different from the other years during the upwelling season, there is no significant variability from year to year and from month to month. The surface NCP values are scattered around the mean with slightly lower estimates for NCP based on oxygen suggesting that the PQ value of 1.4 is too high. These NCP values are calculated during short periods of time when there is biological activity. However, there are periods when no biological activity occurs or when remineralization dominates. This implies that these estimates are upper estimates and that the mean NCP over the whole time series is lower.

4.2. Long-Term Oxygen Biological Production

[34] The detection of O_2 or DIC gradients and the constraint on advection limit the calculation of NCP to a few periods over the whole time series. In order to derive an estimate of the mean biological activity in surface waters at this site, oxygen biological production has been determined using the method described by *Emerson et al.* [2008] and applied at the Hawaii Ocean time series (HOT) station. Equation (8) is used to estimate the biological production rate over the whole time series by calculating the other terms of the equation.

[35] The coarse vertical resolution of temperature does not allow an accurate calculation of the mixed layer depth. Using the available profiles, the mixed layer did not change significantly so the entrainment is neglected (dh/dt = 0)

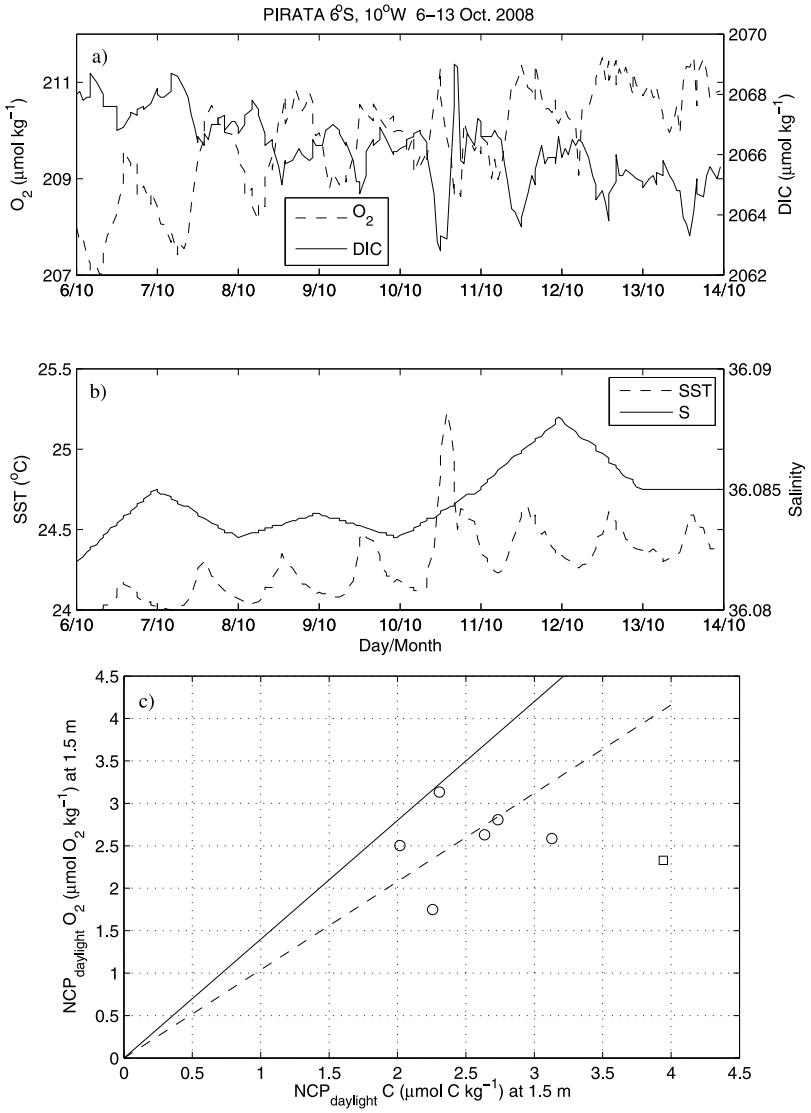

Figure 10. (a) Diurnal cycle of O_2 and DIC and (b) SST and salinity for the 6–13 October 2008. (c) NCP calculated from O_2 (in μmol O_2 kg^{-1}), $NCP_{daylight}O_2$, as a function of NCP calculated from DIC (in μmol C kg^{-1}), $NCP_{daylight}C$. The 10th of October data point is indicated by a square. The solid line corresponds to a ratio of $NCP_{daylight}O_2$ over $NCP_{daylight}C$ of 1.4. The dash line corresponds to mean ratio obtained using the data, except the 10th of October point, and gives a value of 1.0.

and the change of oxygen concentration is assumed to be affected by air-sea exchange, bubbles injection and biological activity. The biological production is then calculated by the difference of all the terms in equation (11). The mixed layer depth is set to 60 m for 2006 and 2009, and to 40 m for 2007 and 2008. The different terms, air-sea O_2 flux, bubbles injection, biological flux and time rate of change in the measured oxygen concentration, are presented as cumulative O_2 flux in mol m^{-2} (Figure 9). The air-sea O_2 flux is an important component but in 2006 it is almost compensated by the bubbles contribution and the biological flux is similar to the observed changes of oxygen concentrations. In 2007, the situation is unusual with a negative biological production. For each year, the biological production is as important as the air-sea O_2 flux. The mean daily net biological oxygen production rates converted to carbon production, using a ratio of 1.4, are 9.4 mmol C m^{-2}d^{-1} for 2006, −10.9 mmol C m^{-2}d^{-1} for 2007, 7.5 mmol C m^{-2}d^{-1} for 2008 and 15.6 mmol C m^{-2}d^{-1} for 2009 over the period of data. In 2008, the oxygen record is after the upwelling season and the biological production is lower than in 2006 and 2009. The net biological oxygen production is significantly different from year to year at this location.

4.3. Determination of the Photosynthetic Quotient (PQ)

[36] Oxygen production is converted to carbon consumption assuming a photosynthetic quotient of 1.4 [*Laws*, 1991]. Simultaneous values of carbon-based and oxygen-based NCP allow the calculation of the photosynthetic quotient. Biological activity starts at sunrise and a diurnal mixed layer is formed during the day until the temperature maximum is reached. Then, the solar radiation decreases, causing cooling and mixed layer depth deepening as a consequence of nocturnal convection. Between sunrise and the SST maximum,

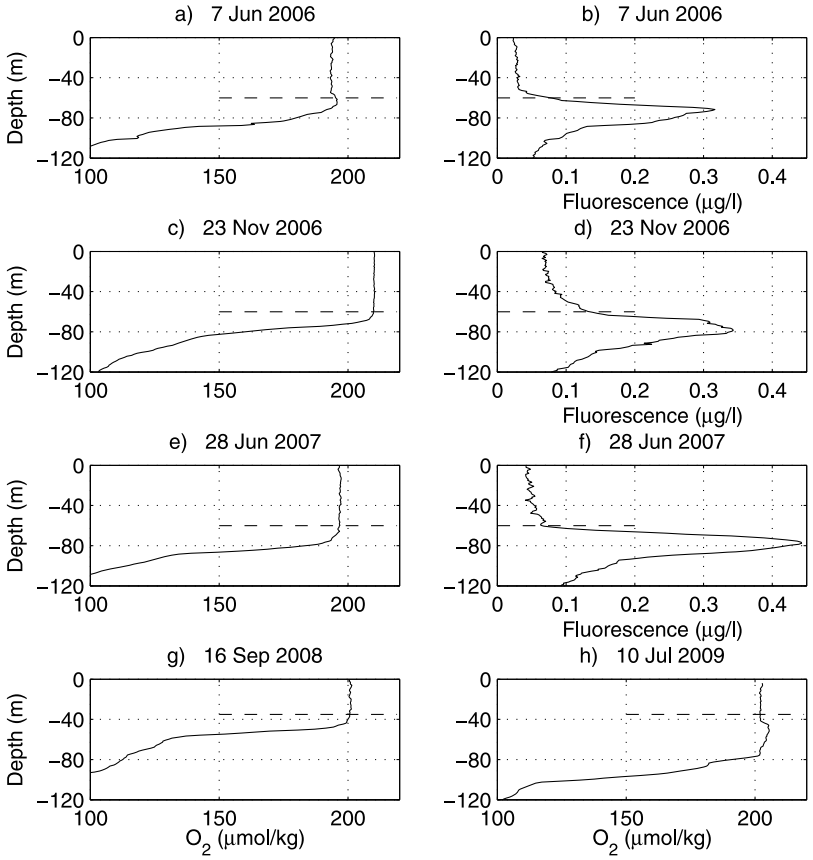

Figure 11. (a) Oxygen and (b) fluorescence profiles at 6°S, 10°W from the CTD on the 7th of June 2006, (c) oxygen and (d) fluorescence profiles on the 23rd of November 2006, (e) oxygen and (f) fluorescence profiles on the 28th of June 2007, and oxygen profiles on (g) the 16th of September 2008 and (h) on the 10th of July 2009. The dash line corresponds to the depth of the mixed layer.

O_2 increases and DIC decreases due to biological activity. During 6–13 October 2008, both O_2 and DIC could be used to calculate NCP during daylight following the method of *Boutin and Merlivat* [2009]. The increase of O_2 and the decrease of DIC occur at the same time (Figure 10a) and are in phase with SST (Figure 10b), which suggests that the DIC variability is dominated by biological activity during that period. The maximum SST is observed later than the statistical maximum of the time series and SST increases over the 7 day period. Over this period, no mixing occurs and the mean alkalinity is constant with a value of 2368.4 $\pm$ 0.1 μmol/kg as salinity is constant (Figure 10b). In addition to biological uptake, air-sea O_2 and CO_2 exchanges occur at the air-sea interface. After removing the contribution of gas exchange, the biological uptake corresponds to the NCP during daylight. For each day, $NCP_{daylight}$ can be calculated from O_2, $NCP_{daylight}$ O_2, and from DIC, $NCP_{daylight}$ C, between sunrise and the SST maximum. $NCP_{daylight}$ O_2 is plotted as a function of $NCP_{daylight}$ C to determine the photosynthetic quotient (Figure 10c). The solid line corresponds to a PQ value of 1.4. The data points are scattered below this line and the 10th of October (indicated by a square) seems to be an outlier. On the 10th of October, a sudden peak of DIC is associated with a larger than 1°C increase within a few hours without any salinity change (Figure 10b). The $NCP_{daylight}$ C is affected by the anomaly of DIC. A linear regression with all the data points gives a PQ value of 0.98 $\pm$ 0.22 and 1.0 $\pm$ 0.2 if the 10th of October value is removed. In Table 2, NCP is calculated with oxygen and DIC for the 6–13 October 2008 and 11–14 November 2009 periods. The NCP based on oxygen is converted in carbon units using a PQ of 1.4. Using the original values of oxygen NCP, a PQ of 1.3 and 1.2 is calculated for the 2008 and 2009 periods respectively.

5. Discussion

[37] Although NCP estimates based on carbon and on oxygen are in reasonable agreement, the NCP based on oxygen tend to be lower values when a PQ of 1.4 is used. From our estimates the PQ ranges from 1.0 to 1.3. The Redfield ratio O_2:DIC is 1.3 (138:106) but the value commonly used is 1.4 [*Laws,* 1991]. *Johnson* [2010], using simultaneous measurements of O_2 and DIC, at two moorings M1 and M2 off Monterey Bay, in California, found -0.77 ± 0.02 and -0.93 ± 0.03 respectively for the O_2: TCO_2 ratio. He explains these low values by the different impact of gas exchange on DIC and O_2, the gas exchange for O_2 being 10 times faster than for CO_2. Our calculations indicate that even after taking into account the gas exchange the O_2:TCO_2 tends to be slightly lower than the Redfield ratio or than the PQ of 1.4. During four visits at a station above the

Table 3. Estimates of Net Community Production in mmol C $m^{-2}d^{-1}$ for Tropical and Subtropical Oceanic Regions[a]

Region	NCP	Method	Reference
PIRATA time series 6°S, 10°W	16.6[b]	O_2, DIC drawdown	this study
PIRATA time series 6°S, 10°W	7.5 to 15.6	O_2 mass balance	this study
Bermuda Time series Station (BATS)	3.8 to 5.9	O_2/ Ar	*Luz and Barkan* [2009]
Sargasso Sea	2.8 ± 4.3	1-D model	*Mouriño-Carballido and Anderson* [2009]
European Time series Station (ESTOC)	5.5 to 13.7	DIC drawdown	*Neuer et al.* [2007]
Hawaii Ocean time series (HOT)	4.3 to 9.3	O_2/N_2	*Emerson et al.* [2008]
Equatorial Pacific	6.9 ± 6.2	Oxygen isotopes	*Hendricks et al.* [2005]
Western equatorial Pacific	4.2 ± 0.6	O_2/ Ar	*Stanley et al.* [2010]
Subtropical Pacific	7.1 ± 1.6	$^{13}C/^{12}C$ of DIC	*Quay et al.* [2009]
Equatorial Pacific	9.3 ± 1.6	$^{13}C/^{12}C$ of DIC	*Quay et al.* [2009]
Hawaii Ocean time series (HOT)	10.0 ± 2.8	O_2/Ar	*Quay et al.* [2010]

[a]NCP calculated from O_2 (mmol O_2 $m^{-2}d^{-1}$) was divided by 1.4 to convert NCP in carbon units (mmol C $m^{-2}d^{-1}$).
[b]This value is obtained by averaging short-term events of biological activity from 2006 to 2009.

Kerguelen plateau, *D. Lefèvre et al.* [2008] measured a PQ value ranging from 0.77 ± 0.28 to 1.26 ± 0.66. This suggests that this ratio is very variable.

[38] The NCP calculated over a few days gives higher values than the mean daily net oxygen production rate deduced from the cumulated fluxes. This is expected as NCP can vary from day to day depending on the cloud cover, the nutrient supply and the photosynthetic available radiation (PAR). This explains the range of NCP values obtained by these high frequency net autotrophic events. The cumulated fluxes correspond to the mean biological production over the length of the time series. Over the time series, the biological production does not follow a linear trend, which shows that there are periods of no biological activity and periods of dominant remineralization, i.e., decreasing biological production (Figure 9). The important contribution to NCP of high frequency events was previously noticed by *Karl et al.* (2003). In addition, the cumulated fluxes are calculated assuming no variability of the mixed layer mixing over the whole time series. Examining the oxygen vertical profiles made at the time of the deployment of the mooring, the water below the mixed layer appears to have lower oxygen concentrations (Figure 11) although a subsurface chlorophyll maximum occurs. A deepening of the mixed layer would then bring oxygen poor water to the surface so the biological production estimated by the mass balance approach underestimates the mean daily production rate. In 2008, the MLD was taken constant at 40 m, a value of 60 m would increase the biological production from 7.5 mmol C $m^{-2}d^{-1}$ to 8 mmol C $m^{-2}d^{-1}$. On the contrary, a shoaling of the mixed layer from 60 m to 40 m would reduce the biological production by 24% in 2006 and by 4.5% in 2009.

[39] Another term that has been neglected in both calculations is the vertical diffusion flux K_z:

$$F_z = K_z \frac{d[O_2]}{dz} \tag{13}$$

where K_z is the diffusion coefficient. Its value for stratified water is about 4.1 10^{-6} m^2 s^{-1} [*Denman and Gargett*, 1983]. From the available vertical profiles of oxygen down to 120 m (Figure 11), the vertical gradient of oxygen is about −0.89 mmol m^{-4}. This leads to a diffusion flux of −0.31 mmol $m^{-2}d^{-1}$, which is small compared to the total air-sea O_2 flux of about 15 mmol $m^{-2}d^{-1}$ (Figure 6a) and to the mean NCP ranging from 7.5 to 15.6 mmol $m^{-2}d^{-1}$.

[40] The gas exchange coefficient is also a source of uncertainty and would have an impact on the air-sea flux. However, as the air-sea flux of O_2 and the bubble flux are in opposite direction, the error on the gas exchange coefficient would have a smaller impact on the estimate of the biological production. For example, decreasing both fluxes by 10% would lead to a biological production of 9.2 mmol $m^{-2}d^{-1}$ instead of 9.4 mmol $m^{-2}d^{-1}$ in 2006, whereas decreasing only the air-sea O_2 flux by 10% would give 8.6 mmol $m^{-2}d^{-1}$.

[41] In 2007, the mass balance approach gives a negative biological production rate because the site is undersaturated in oxygen whereas the oxygen distribution is above the saturation level for the other years. As there is no significant difference between the upwelling in 2007 compared to the other years [*Caniaux et al.*, 2011], it is difficult to explain this feature and it might be due to a problem with the measurements. Nevertheless, oxygen concentrations increase during the upwelling season showing that biological activity also occurs in 2007. The site is located in the eastern tropical Atlantic (ETRA) where *Serret et al.* [2001] observed heterotrophy with O_2 supersaturated waters along an Atlantic Meridional Transect (15°S-14°N) in May–June 1998. They measured respiration and gross primary production and found higher respiration rate than production rate. These measurements are necessarily very local and correspond to a situation at a given time. *Neuer et al.* [2007], sampling at a monthly scale, from 1994 to 2000, at the European time series station ESTOC, always found positive NCP, which contradicts reports of a heterotrophic subtropical North East Atlantic.

[42] *Robinson et al.* [2002] tried to provide temporal context to the measurements made along an Atlantic Meridional Transect by examining oxygen fluxes such as those published by *Najjar and Keeling* [2000] and *Boyer et al.* [1999]. However, seasonal and annual patterns of oxygen fluxes do not allow a differentiation between plankton respiration and upwelling or deep winter mixing.

[43] For 2006, 2008 and 2009, when surface waters are supersaturated in oxygen, our biological production obtained over the whole time series, is in good agreement with those reported for tropical and subtropical regions (Table 3) given the observed variability. *Emerson et al.* [2008] found significant year to year variability at the HOT site in 1997, 1998 and 2005 (Table 3). Such variability was also reported for the ESTOC site from 1995 to 2000 (Table 3). Our estimates

tend to be slightly higher but they are quite close to those given further north in the eastern Atlantic at ESTOC, 29.16°N, 15.5°W. Further west of ESTOC but at the same latitude, estimates at BATS yield lower values.

6. Summary and Conclusions

[44] Hourly oxygen and CO_2 measurements have been made since 2006 at the PIRATA mooring at 6°S, 10°W. The site is characterized by a decrease in surface temperature from June to September, as a result of equatorial and coastal upwelled water propagating to the mooring site. The surface water is supersaturated in oxygen except in 2007 when undersaturation is observed during the upwelling season. However, the concentration of oxygen increases throughout the upwelling period suggesting that biological production dominates. Using an alkalinity-salinity relationship, dissolved inorganic carbon can be calculated from the fugacity of CO_2 and alkalinity. Net community production is calculated from changes of DIC and/ or O_2 over short periods of time when biological activity is present and no mixing is encountered. Most of the NCP values are obtained from June to December and averaging all the values leads to an NCP value of 16.6 ± 6.1 mmol C $m^{-2}d^{-1}$. Over the 6–13 October 2008 period, concomitant O_2 and DIC decreases allow the calculation of the photosynthetic quotient. The value of 1.0 ± 0.2 is slightly lower than the 1.4 theoretical value generally used.

[45] As expected, the mean NCP value corresponding to short bursts of biological production is higher than the mean daily oxygen production determined over the whole time series, assuming negligible vertical mixing and horizontal advection. As the mooring site is located outside the upwelling area, assuming no significant mixed layer deepening is a reasonable assumption. However, the site is affected by horizontal advection. This process can be neglected for oxygen when air-sea exchange occurs at a faster rate than horizontal advection. The mean daily oxygen production shows a significant year to year variability with values of 9.4 mmol C $m^{-2}d^{-1}$ in 2006, 7.5 mmol C $m^{-2}d^{-1}$ in 2008 and 15.6 mmol C $m^{-2}d^{-1}$ in 2009. Our estimates are in good agreement with those determined at ESTOC and tend to be slightly higher than those reported for the Pacific ocean. However, given the year to year variability in all the estimates, it is difficult to determine whether this is a permanent feature. Our NCP measurements as well as the increasing trend of oxygen concentrations suggest an autotrophic situation at our site. Despite the uncertainties and the assumptions made to calculate NCP, the consistency between the estimates based on carbon and oxygen data suggests that biological production can be determined by monitoring O_2 and CO_2 at this site.

[46] **Acknowledgments.** This work was funded by the European Integrated Project CARBOOCEAN (contract 511176–2), the Institut de Recherche pour le Développement (IRD) and the national program LEFE CYBER. Data management for PIRATA moorings is conducted by the TAO project office at NOAA/PMEL in collaboration with many research institutes listed on the PIRATA website (http://www.pmel.noaa.gov/pirata). We are grateful to Laurence Beaumont, Théo Danguy and Antoine Guillot from DT INSU for their technical support with the CO_2 and O_2 sensors, and the U.S. IMAGO of IRD for their help with mooring deployments. We thank two anonymous reviewers for their helpful comments that contributed to improve the manuscript.

References

Bourlès, B., et al. (2008), The PIRATA program: History, accomplishments and future directions, *Bull. Am. Meteorol. Soc.*, *89*, 1111–1125, doi:10.1175/2008BAMS2462.1.

Boutin, J., and L. Merlivat (2009), New in situ estimates of carbon biological production rates in the Southern Ocean from CARIOCA drifter measurements, *Geophys. Res. Lett.*, *36*, L13608, doi:10.1029/2009GL038307.

Boyer, T., M. E. Conkright, and S. Levitus (1999), Seasonal variability of dissolved oxygen, percent oxygen saturation, and apparent oxygen utilization in the Atlantic and Pacific Oceans, *Deep Sea Res., Part I*, *46*, 1593–1613, doi:10.1016/S0967-0637(99)00021-7.

Caniaux, G., H. Giordani, J.-L. Redelsperger, F. Guichard, E. Key, and M. Wade (2011), Coupling between the Atlantic cold tongue and the West African monsoon in boreal spring and summer, *J. Geophys. Res.*, *116*, C04003, doi:10.1029/2010JC006570.

Denman, K. L., and A. E. Gargett (1983), Time and space scales of vertical mixing and advection of phytoplankton in the upper ocean, *Limnol. Oceanogr.*, *28*(5), 801–815, doi:10.4319/lo.1983.28.5.0801.

Dickson, A. G., and F. J. Millero (1987), A comparison of the equilibrium constants for the dissociation of carbonic acid in seawater media, *Deep Sea Res.*, *34*, 1733–1743, doi:10.1016/0198-0149(87)90021-5.

Emerson, S., and C. Stump (2010), Net biological oxygen production in the ocean—II: Remote in situ measurements of O_2 and N_2 in subarctic pacific surface waters, *Deep Sea Res., Part I*, *57*, 1255–1265, doi:10.1016/j.dsr.2010.06.001.

Emerson, S., P. D. Quay, D. M. Karl, C. D. Winn, L. Tupas, and M. R. Landry (1997), Experimental determination of the organic carbon flux from open-ocean surface waters, *Nature*, *389*, 951–954, doi:10.1038/40111.

Emerson, S., C. Stump, and D. Nicholson (2008), Net biological oxygen production in the ocean: Remote in situ measurements of O_2 and N_2 in surface waters, *Global Biogeochem. Cycles*, *22*, GB3023, doi:10.1029/2007GB003095.

García, H. E., and L. I. Gordon (1992), Oxygen solubility in seawater: Better fitting equations, *Limnol. Oceanogr.*, *37*(6), 1307–1312, doi:10.4319/lo.1992.37.6.1307.

Garcia, H. E., and R. F. Keeling (2001), On the global oxygen anomaly and air-sea flux, *J. Geophys. Res.*, *106*(C12), 31,155–31,166, doi:10.1029/1999JC000200.

Hendricks, M., M. L. Bender, B. A. Barnett, P. Strutton, and F. P. Chavez (2005), Triple oxygen isotopes composition of dissolved O_2 in the equatorial Pacific: A tracer of mixing, production, and respiration, *J. Geophys. Res.*, *110*, C12021, doi:10.1029/2004JC002735.

Johnson, K. S. (2010), Simultaneous measurements of nitrate, oxygen, and carbon dioxide on oceanographic moorings: Observing the Redfield ratio in real time, *Limnol. Oceanogr.*, *55*(2), 615–627, doi:10.4319/lo.2009.55.2.0615.

Kaiser, J., M. K. Reuer, B. A. Barnett, and M. L. Bender (2005), Marine productivity estimates from continuous O_2/Ar ratio measurements by membrane inlet mass spectrometry, *Geophys. Res. Lett.*, *32*, L19605, doi:10.1029/2005GL023459.

Karl, D. M., E. A. Laws, P. Morris, P. J. B. Williams, and S. Emerson (2003), Metabolic balance of the open sea, *Nature*, *426*, 32, doi:10.1038/426032a.

Laws, E. A. (1991), Photosynthetic quotients, new production and net community production in the open ocean, *Deep Sea Res.*, *38*, 143–167, doi:10.1016/0198-0149(91)90059-O.

Lefèvre, D., C. Guigue, and I. Obernosterer (2008), The metabolic balance at two constrasting sites in the Southern Ocean: The iron-fertilized Kerguelen area and HNLC waters, *Deep Sea Res.*, *55*(5–7), 766–776, doi:10.1016/j.dsr2.2007.12.006.

Lefèvre, N., A. Guillot, L. Beaumont, and T. Danguy (2008), Variability of fCO_2 in the Eastern Tropical Atlantic from a moored buoy, *J. Geophys. Res.*, *113*, C01015, doi:10.1029/2007JC004146.

Luz, B., and E. Barkan (2009), Net and gross oxygen production from O_2/Ar, $^{17}O/^{16}O$ and $^{18}O/^{16}O$ ratios, *Aquat. Microb. Ecol.*, *56*, 133–145, doi:10.3354/ame01296.

McNeil, C. L., and D. M. Farmer (1995), Observations of the influence of diurnal convection on upper ocean dissolved gas measurements, *J. Mar. Res.*, *53*, 151–169, doi:10.1357/0022240953213313.

Mehrbach, C., C. H. Culberson, J. E. Hawley, and R. M. Pytkowicz (1973), Measurement of the apparent dissociation constants of carbonic acid in seawater at atmospheric pressure, *Limnol. Oceanogr.*, *18*, 897–907, doi:10.4319/lo.1973.18.6.0897.

Merlivat, L., M. Gonzalez Davila, G. Caniaux, J. Boutin, and G. Reverdin (2009), Mesoscale and diel to monthly variability of CO_2 and carbon fluxes at the ocean surface in the northeastern Atlantic, *J. Geophys. Res.*, *114*, C03010, doi:10.1029/2007JC004657.

Mouriño-Carballido, B., and L. A. Anderson (2009), Net community production of oxygen derived from in vitro and in situ 1-D modeling

techniques in a cyclonic mesoscale eddy in the Sargasso Sea, *Biogeosciences*, *6*, 1799–1810, doi:10.5194/bg-6-1799-2009.

Najjar, R. G., and R. F. Keeling (2000), Mean annual cycle of the air-sea oxygen flux: A global view, *Global Biogeochem. Cycles*, *14*, 573–584, doi:10.1029/1999GB900086.

Neuer, S., et al. (2007), Biogeochemistry and hydrography in the eastern subtropical North Atlantic gyre. Results from the European time-series station ESTOC, *Prog. Oceanogr.*, *72*, 1–29, doi:10.1016/j.pocean.2006.08.001.

Parard, G., N. Lefèvre, and J. Boutin (2010), Sea water fugacity of CO_2 at the PIRATA mooring at 6°S, 10°W, *Tellus, Ser. B*, *62*(5), 636–648, doi:10.1111/j.1600-0889.2010.00503.x.

Quay, P. D., J. Stutsman, R. A. Feely, and L. W. Juranek (2009), Net community production rates across the subtropical and equatorial Pacific ocean estimated from air-sea $\delta^{13}C$ disequilibrium, *Global Biogeochem. Cycles*, *23*, GB2006) doi:10.1029/2008GB003193.

Quay, P. D., C. Peacock, K. Björkman, and D. M. Karl (2010), Measuring primary production rates in the ocean: Enigmatic results between incubation and non-incubation methods at Station ALOHA, *Global Biogeochem. Cycles*, *24*, GB3014, doi:10.1029/2009GB003665.

Robinson, C., P. Serret, G. Tilstone, E. Teira, M. V. Zubkov, A. P. Rees, and E. M. S. Woodward (2002), Plankton respiration in the Eastern Atlantic Ocean, *Deep Sea Res., Part I*, *49*, 787–813, doi:10.1016/S0967-0637(01)00083-8.

Serret, P., C. Robinson, E. Fernández, E. Teira, and G. Tilstone (2001), Latitudinal variation of the balance between plankton photosynthesis and respiration in the eastern Atlantic Ocean, *Limnol. Oceanogr.*, *46*(7), 1642–1652, doi:10.4319/lo.2001.46.7.1642.

Stanley, R. H. R., W. J. Jenkins, D. E. Lott III, and S. C. Doney (2009), Noble gas constraints on air-sea gas exchange and bubble fluxes, *J. Geophys. Res.*, *114*, C11020, doi:10.1029/2009JC005396.

Stanley, R. H. R., J. B. Kirkpatrick, N. Cassar, B. A. Barnett, and M. L. Bender (2010), Net community production and gross primary production rates in the western equatorial Pacific, *Global Biogeochem. Cycles*, *24*, GB4001, doi:10.1029/2009GB003651.

Sweeney, C., E. Gloor, A. R. Jacobson, R. M. Key, G. McKinley, J. L. Sarmiento, and R. Wanninkhof (2007), Constraining global air-sea gas exchange for CO_2 with recent bomb ^{14}C measurements, *Global Biogeochem. Cycles*, *21*, GB2015, doi:10.1029/2006GB002784.

Wade, M., G. Caniaux, Y. Dupenhoat, M. Dengler, H. Giordani, and R. Hummels (2011), A one dimensional modelling study of the diurnal cycle in the tropical Atlantic at the PIRATA buoys during the EGEE-3 campaign, *Ocean Dyn.*, *61*, 1–20, doi:10.1007/s10236-010-0337-8.

Wanninkhof, R. H. (1992), Relationship between wind speed and gas exchange over the ocean, *J. Geophys. Res.*, *97*(C5), 7373–7382, doi:10.1029/92JC00188.

Weiss, R. F. (1974), CO_2 in water and seawater: The solubility of a non-ideal gas, *Mar. Chem.*, *2*, 203–215, doi:10.1016/0304-4203(74)90015-2.

Weiss, R. F., and B. A. Price (1980), Nitrous oxide solubility in water and seawater, *Mar. Chem.*, *8*, 347–359, doi:10.1016/0304-4203(80)90024-9.

Woolf, D. K., and S. A. Thorpe (1991), Bubbles and the air-sea exchange of gases in near-saturation conditions, *J. Mar. Res.*, *49*, 435–466, doi:10.1357/002224091784995765.

N. Lefèvre and L. Merlivat, LOCEAN, UMR7159, Université Pierre et Marie Curie, CNRS, IRD, MNHN, 4 Place Jussieu, case 100, Tour 45-46, 5ème étage, F-75252 Paris CEDEX 05, France. (nathalie.lefevre@locean-ipsl.upmc.fr)